https://doi.org/10.1093/plphys/kiac299 PLANT PHYSIOLOGY 2022: 190: 562–575

Plant Physiology®

Research Article

A myosin XI adaptor, TAPE, is essential for pollen tube elongation in rice

Woo-Jong Hong [1], Eui-Jung Kim [1], Jinmi Yoon [2], Jeniffer Silva [1], Sunok Moon [1], Cheol Woo Min [2], Lae-Hyeon Cho,[2] Sun Tae Kim,[2] Soon Ki Park [3], Yu-Jin Kim [4,*] and Ki-Hong Jung [1,*]

1 Graduate School of Green-Bio Science & Crop Biotech Institute, Kyung Hee University, Yongin, 17104, Republic of Korea
2 Department of Plant Bioscience, Pusan National University, Miryang, 50463, Republic of Korea
3 School of Applied Biosciences, Kyungpook National University, Daegu, 41566, Republic of Korea
4 Department of Life Science and Environmental Biochemistry, Pusan National University, Miryang, 50463, Republic of Korea

*Authors for correspondence: yjkim2020@pusan.ac.kr (Y.-J.K.); khjung2010@khu.ac.kr (K.-H.J.)

W.-J.H., Y.-J.K., and K.-H.J. designed the study. W.-J.H., Y.-J.K., E.-J.K., J.Y., J.S., S.M., C.W.M., and L.-H.C. performed experiments. W.-J.H., Y.-J.K., S.T.K., S.K.P., and K.-H.J. analyzed data. W.-J.H., Y.-J.K., and K.-H.J. wrote the manuscript and all authors reviewed the final manuscript.

The author responsible for distribution of materials integral to the findings presented in this article in accordance with the policy described in the Instructions for Authors (https://academic.oup.com/plphys/pages/general-instructions) are: Yu-Jin Kim (yjkim2020@pusan.ac.kr) and Ki-Hong Jung (khjung2010@khu.ac.kr).

Abstract

Pollen tube (PT) elongation is important for double fertilization in angiosperms and affects the seed-setting rate and, therefore, crop productivity. Compared to Arabidopsis (*Arabidopsis thaliana* L.), information on PT elongation in rice (*Oryza sativa* L.) is limited by the difficulty in obtaining homozygous mutants. In a screen of T-DNA insertional mutants, we identified a mutant in the *Tethering protein of actomyosin transport in pollen tube elongation* (*TAPE*) gene with an unusual segregation ratio by genotyping analysis. A CRISPR/Cas9 knockout mutant of *TAPE* that produced a short PT was sterile, and *TAPE* was expressed specifically in pollen grains. TAPE is a homolog of a myosin XI adaptor in Arabidopsis with three tetratricopeptide repeat and Phox and Bem1 protein domains. TAPE showed latrunculin B-sensitive, actin-dependent localization to the endoplasmic reticulum. Yeast two-hybrid screening and transcriptome analysis revealed that TAPE interacted with pollen-specific LIM protein 2b and elongation factor 1-alpha. Loss of *TAPE* affected transcription of 1,259 genes, especially genes related to cell organization, which were downregulated. In summary, *TAPE* encodes a myosin XI adaptor essential for rice PT elongation.

Introduction

Pollen tube (PT) elongation, an essential process for successful sexual reproduction in angiosperms, is a model system for rapid polar growth (Kroeger and Geitmann, 2012). After pollination, pollen grains attach to the stigma, become hydrated (Moon and Jung, 2020), germinate, and elongate the PT into the transmitting tract in the pistil. The immotile male gametes (two sperm cells and a generative cell), initially released into the ovule via a delicately controlled PT, fuse with and fertilize the egg cell and central cell (Johnson et al., 2019).

Several PT elongation genes have been studied in Arabidopsis (*Arabidopsis thaliana* L.). Two *Catharanthus roseus* receptor-like kinase (CrRLKs) family proteins, Buddha's Paper Seal 1 (BUPS1) and BUPS2 have redundant roles in normal PT elongation in the pistil (Zhu et al., 2018).

Received March 23, 2022. Accepted May 30, 2022. Advance access publication June 23, 2022

The CrRLKs interact with Rho-of-plants guanine nucleotide exchange factors (RopGEFs), and a mutation of the RopGEFs resulted in depolarized growth of the PT in the pistil. Along with the two CrRLKs, rapid alkalinization factors (RALFs) are also involved in PT elongation. Pollen-expressed peptides, RALF4 and RALF19 interact with leucine-rich repeat extensin to control PT integrity during elongation (Mecchia et al., 2017). In addition, LORELEI-like GPI-anchored protein 2 (LLG2) and LLG3 control PT growth via the interaction of ANXUR and BUPS in a RALF4-dependent manner (Feng et al., 2019). A Rho-type GTPase of plants, ROP1 in Arabidopsis is a key regulator for establishing the polarity in PT growth, which is coupled to Ca^{2+} influx and actin filament (AF) dynamics (Li et al., 1999; Gu et al., 2003). Additional genes involved in AF organization (Xu and Huang, 2020), cell wall integrity (Chen and Ye, 2007; Vogler et al., 2019), and ion gradient (Michard et al., 2017; Hoffmann et al., 2020) are required for PT elongation.

Actomyosin-dependent transport mediated by the AF-related motor protein myosin is not only in plant organelle transport generating cytoplasmic streaming (Ross et al., 2008; Tominaga and Ito, 2015) but also in PT elongation (Cai and Cresti, 2009; Madison et al., 2015). In Arabidopsis, there are 17 myosins, classified into two subgroups, four myosins in class VIII and 13 myosins in class XI (Avisar et al., 2009). These plant-specific myosins resemble vertebrate myosin V, consisting of a motor domain, six IQ motifs, a coiled-coil domain, and a C-terminal globular tail domain (GTD) (Tominaga and Nakano, 2012). Due to its high velocity, with a 35-nm step size (Tominaga et al., 2003), myosin XI is important for the motility of organelles such as the endoplasmic reticulum (ER), nucleus, Golgi stacks, peroxisomes, and mitochondria (Ueda et al., 2015). For example, myosin XI-K is involved in ER motility, and AF bundle organization depends on interactions with myosin XI-2 (Ueda et al., 2010). Myosin XI-I localizes on the nuclear membrane and moves to the nucleus via interaction with WPP domain-interacting tail-anchored protein 1 (WIP1) and WIP2 (Tamura et al., 2013). In addition, myosin XI-C and myosin XI-E mediate Golgi stacks, peroxisomes, and mitochondrial movement along with secretory vesicle transport in Arabidopsis PT (Wang et al., 2020). Two myosin XI receptors, myosin-binding protein 1 (MyoB1) and MyoB2, identified by a yeast two-hybrid (Y2H) screening assay using the GTD of myosin XI, contain a transmembrane domain and a domain of unknown function 593 (DUF593) (Peremyslov et al., 2013). They are involved in vesicular cargo transport together with myosins XI. In tobacco (*Nicotiana tabacum* L.), RAC/ROP GTPase5 (RAC5) and the DUF593 containing protein, RAC5 interacting subapical PT protein regulate trafficking of the trans-Golgi network in PT growth (Stephan et al., 2014). Two other adaptor families in Arabidopsis, myosin XI adaptors of family A (MadA) and MadB, have four members in each family (Kurth et al., 2017). Although their role in PT elongation is unknown, mutants with multiple MadB knockout (KO) genes show a progressive reduction in root hair length with increasing numbers of MadB KO genes.

Rice (*Oryza sativa* L.) is an important crop plant that supplies calories for almost half of mankind. Unlike Arabidopsis, rice has an ovule in a carpel; therefore, there has been little characterization of rice genes related to pollen germination and PT elongation (Kim et al., 2019b). Using genome editing to generate homozygous (HM) KO mutants at the T_0 generation, several genes involved in rice PT elongation have been identified. Ruptured PT and Male-gene transfer defective 2, members of the CrRLK family in rice, maintain PT integrity by interacting with K^+ transporters and by balancing reactive oxygen species, respectively (Liu et al., 2016; Kim et al., 2021b). In addition, Germinating modulator of rice pollen and its downstream interactor, an AP180 N-terminal homology (ANTH) domain-containing protein, OsANTH3 affect PT growth in rice by regulating clathrin-mediated endocytosis (Kim et al., 2021a; Lee et al., 2021). Although actomyosin transport is important in the PT elongation process and 14 class XI myosins were identified in rice (Jiang and Ramachandran, 2004), the mechanism of PT elongation is unknown.

Here, we report a gene, *Tethering protein of actomyosin transport in PT elongation* (*TAPE*), which encodes a myosin XI adaptor essential for PT elongation in rice. We present a regulatory model of *TAPE* in PT elongation that is supported by various experimental evidence and characterize a myosin XI adaptor in PT elongation. This information could be useful in understanding the actomyosin transport mechanism for PT elongation in plants and be used for applications to maintain crop yield.

Results

Identification of *TAPE* and its impact on rice male gamete transmission

From a large-scale T-DNA mutant screening for 627 late pollen-preferred genes (Moon et al., 2018), we identified genes related to gamete gene transfer in rice. A T-DNA insertion line in *TAPE* (2B-00091) had a 1:1 wild-type (WT) to heterozygote (*TAPE/tape*) segregation ratio without HM progeny. We confirmed by genotyping that a T-DNA was located in the intron of *TAPE* on the backside of three tetratricopeptide repeat (TPR) and Phox and Bem1 (PB1) domains (Figure 1A). To determine whether the mutation caused a defect in male or female gamete transfer, we performed reciprocal crosses. The *TAPE/tape* plant as a paternal line (male donor) crossed with the WT produced only *TAPE/TAPE* progeny. In contrast, when the *TAPE/tape* plant was the maternal line (female donor), there was almost a 1:1 ratio of *TAPE/TAPE* to *TAPE/tape* progeny (Table 1). Thus, *TAPE* is an essential gene for male gamete transmission.

tape-1 exhibits short PT growth without germination defects

Since we could not obtain the HM mutant of *TAPE* by traditional methods, we generated two independent HM

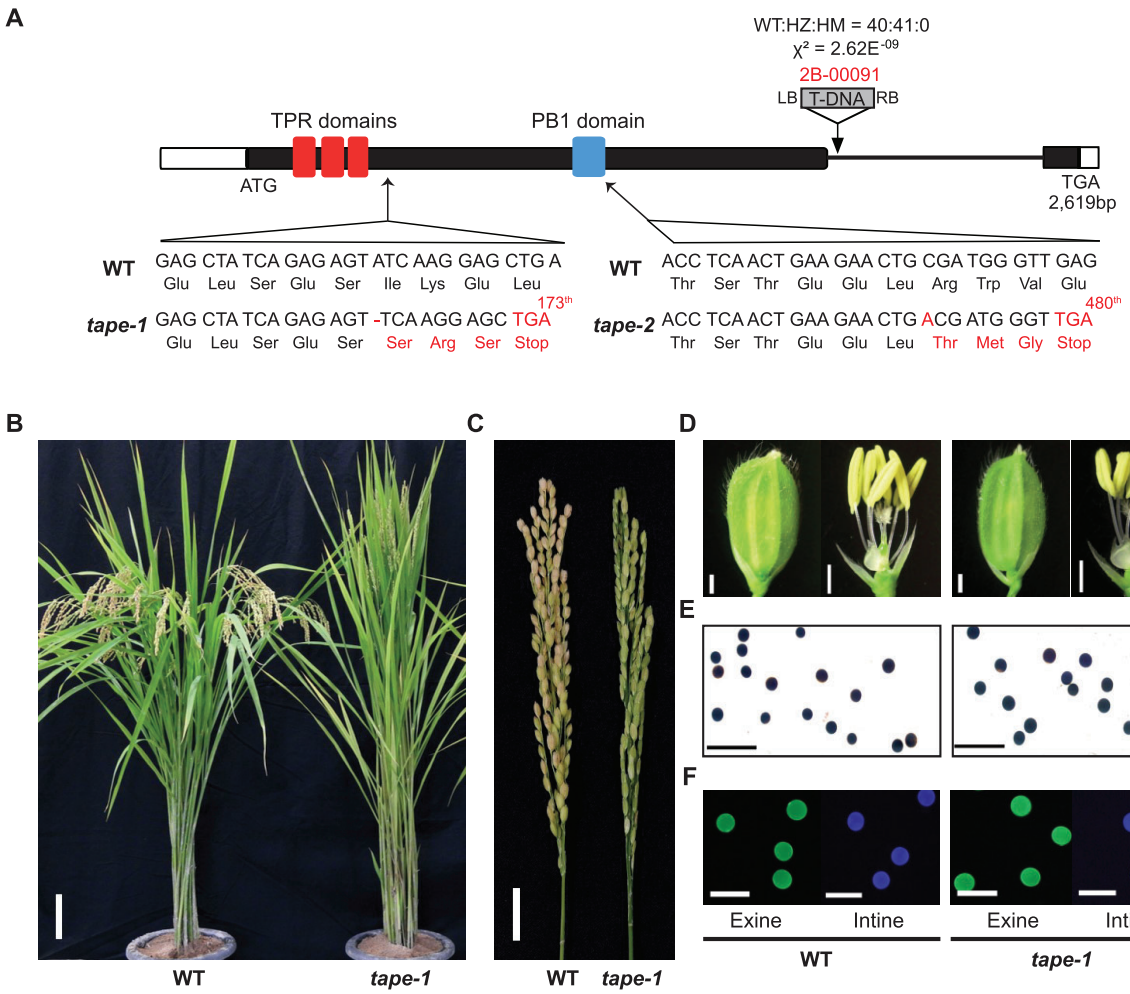

Figure 1 Gene structure of *TAPE* and the phenotype of the *tape-1* mutant. A, Gene structure of *TAPE* and the T-DNA insertion and CRISPR/Cas9 mutants (*tape-1* and *tape-2*). The black and white boxes indicate exon and untranslated regions, respectively. The gray box represents the T-DNA fragment inserted in *TAPE*. The *P*-value from the χ^2 test result compared to the predicted 1:2:1 ratio for the WT:HZ:HM is shown. Red letters indicate insertions or deletions in the *tape-1* and *tape-2* mutants with altered amino acids. B and C, Phenotypes of the WT and *tape-1* plants showing sterility of *tape-1* plants without vegetative growth defects. Bar = 10 cm (B), 2 cm (C). D, Morphology of the spikelet and floret of WT and *tape-1* plants. Bar = 2 mm. E–F, pollen stained with I_2-KI (E), auramine O, or calcofluor white solutions (F) for starch content, and the exine and intine layers of the pollen, respectively. Bar = 200 μm (E), 100 μm (F).

Table 1 Reciprocal crossing assay of *TAPE*

Genotype of Parents		Genotype of Progeny			Expected Ratio	Observed Ratio	χ^2 test (1:1:0)
♀	♂	*TAPE/TAPE* (WT)	*TAPE/tape* (+ /–)	*tape/tape* (–/–)	WT:(+ /–):(–/–)	WT:(+ /–):(–/–)	*P*-value
TAPE/TAPE	*TAPE/tape*	19	0	0	1:1:0	19:0:0	$1.307E^{-0.5}$
♀	♂	*TAPE/TAPE* (WT)	*TAPE/tape* (+ /–)	*tape/tape* (–/–)	WT:(+ /–):(–/–)	WT:(+ /–):(–/–)	*P*-value
TAPE/tape	*TAPE/TAPE*	28	42	0	1:1:0	2:3:0	0.09

mutants (*tape-1* and *-2*) using the CRISPR/Cas9 system and found a sterile phenotype in two independent gene-edited lines (Figure 1, A–C; Supplemental Figure S1, A and B). To determine whether sterility resulted from developmental defects of the anther or pollen, we analyzed the morphology of the anther and pollen in the maturation stage (Figure 1, D–F; Supplemental Figure S1, C–E). The anthers in the WT and two HM strains (*tape-1* and *-2*) both developed normally (Figure 1D; Supplemental Figure S1C). Starch accumulation, seen by staining with I_2-KI, and wall formation in pollen grains, seen by staining with calcofluor white and auramine O for intine and exine layers, respectively, were normal (Figure 1, E and F; Supplemental Figure S1, D and E). Therefore, the sterile phenotypes in the *tape-1* and *tape-2* mutants were not caused by developmental defects of the anther and pollen at the maturation stage.

When we compared *in vitro* pollen germination between the WT and *tape-1* strains, we observed short PTs in the

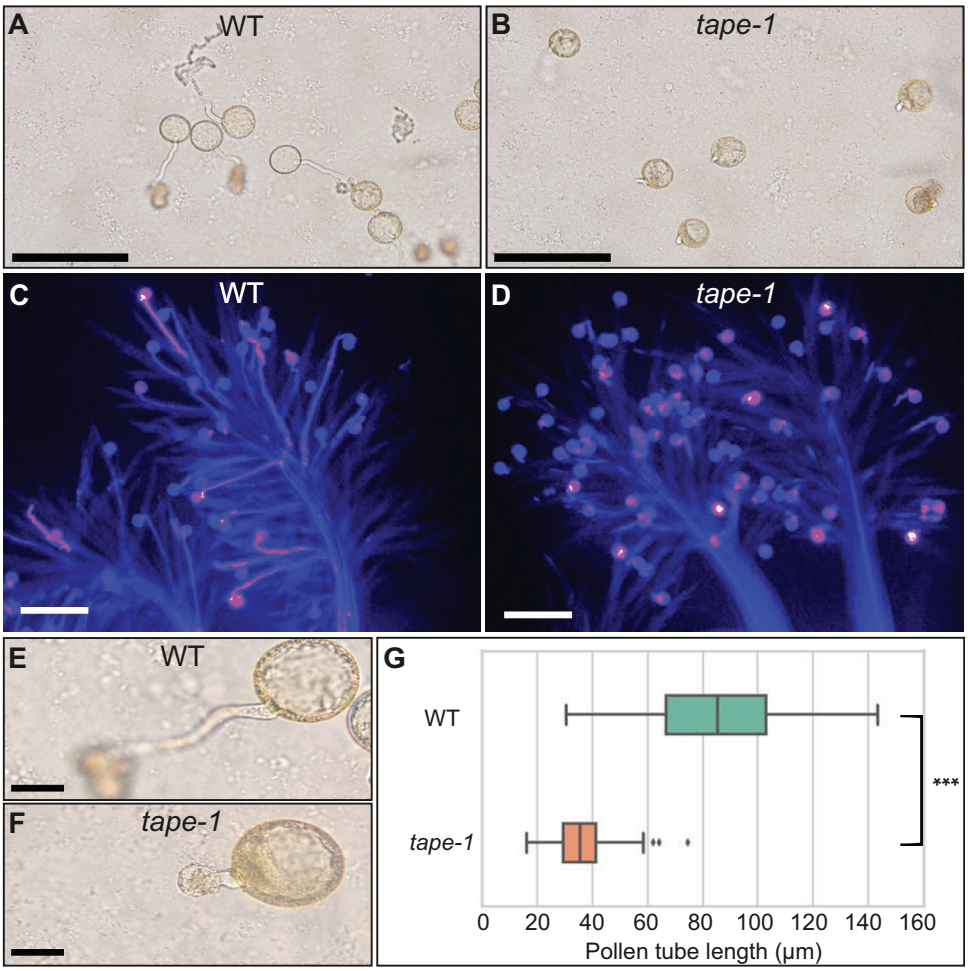

Figure 2 *In vitro* and *in vivo* germination of WT and *tape-1* pollen. A–B, *In vitro* germination of WT and *tape-1* pollen showing the short PTs of *tape-1*. Bar = 200 μm. C–D, *In vivo* germination 2 h after pollination. The *tape-1* pollen did not elongate sufficiently to penetrate the stigma. Bar = 200 μm. E–F, Magnified photograph of fully elongated PTs from the WT compared to *tape-1*. Bar = 20 μm. G, Box plot of PT length in WT and *tape-1*. It indicates upper and lower quartiles, median, and outlier of measured PT length. At least 150 PTs were counted. *** indicates *P*-value < 0.001 calculated from the Student's *t* test.

tape-1 strain compared to the WT (Figure 2, A and B) without substantial differences in the pollen germination rate (Supplemental Figure S2). The short PTs in the *tape-1* strain were also seen in the *in vivo* germination assay using the pistils after 2 h of pollination (Figure 2, C and D). The PTs in the *tape-1* strain were attached and germinated on the stigma but, unlike the WT, did not reach the transmitting track on the style. In the magnified PTs of WT and *tape-1*, the PTs of the *tape-1* strain had a short but intact PT (Figure 2, E and F), which was reduced about 30% in length in *tape-1* (Figure 2G) leading to the male gamete defect. The short PT phenotype was also observed in the *tape-2* allele in both *in vitro* and *in vivo* germination assays (Supplemental Figure S1, F and G).

TAPE is expressed specifically in the pollen grain and PT

We measured gene expression by reverse transcription-quantitative PCR (RT-qPCR) and tissue and developmental expression patterns using a histochemical β-glucuronidase (GUS) assay (Figure 3, A and B). RT-qPCR analysis of nine samples including vegetative tissues, panicle, developing anthers, mature pollen, and developing seeds showed that *TAPE* was expressed specifically in mature pollen at levels 4 times higher than a reference gene, *OsUbi5* (Figure 3A). For plant expression patterns of *TAPE*, we generated a native *TAPE* promoter-driven GUS transgenic plant (*pTAPE::TAPE-GUS*) and performed histochemical analysis during late anther developmental stages (Figure 3B; Zhang et al., 2011). This revealed that *TAPE* was expressed specifically in mature pollen but not in other floret tissues. The expression began after the bicellular pollen stage as predicted by the rice male gamete expression database (Chandran et al., 2020). TAPE-GUS proteins were localized on PTs in the germinated pollen of the *pTAPE::TAPE-GUS* line.

TAPE protein is mainly localized to the ER

To determine the subcellular localization of the TAPE protein, we constructed a C-terminal green fluorescent protein (GFP)-fused TAPE (*p35s::TAPE-GFP*) in a plasmid for a

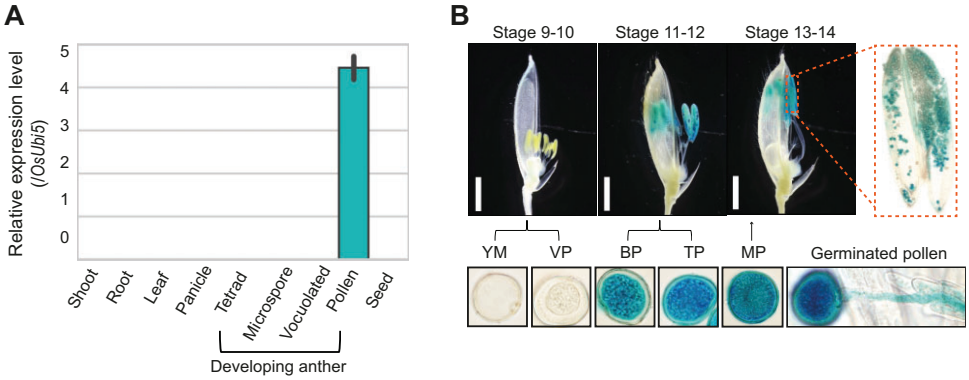

Figure 3 Expression and histochemical assays of *TAPE*. A, Relative *TAPE* expression in various rice tissues and tetrad, microspore, and vacuolated stages of the anther as determined by RT-qPCR. Values are presented as the mean ± standard deviation for three biological replicates, normalized to the reference gene *OsUbi5* (*Os01g22490*) using the $2^{-\Delta\Delta Ct}$ method. B, Florets from the *pTAPE::TAPE-GUS* transgenic plants were stained for GUS expression. Pollen was released from the anther by tweezing with forceps. Bar = 2 mm. Stages above the floret images indicate anther development stages (Zhang et al., 2011). YM, young microspore; VP, vacuolated pollen; BP, bicellular pollen; TP, tricellular pollen; MP, mature pollen.

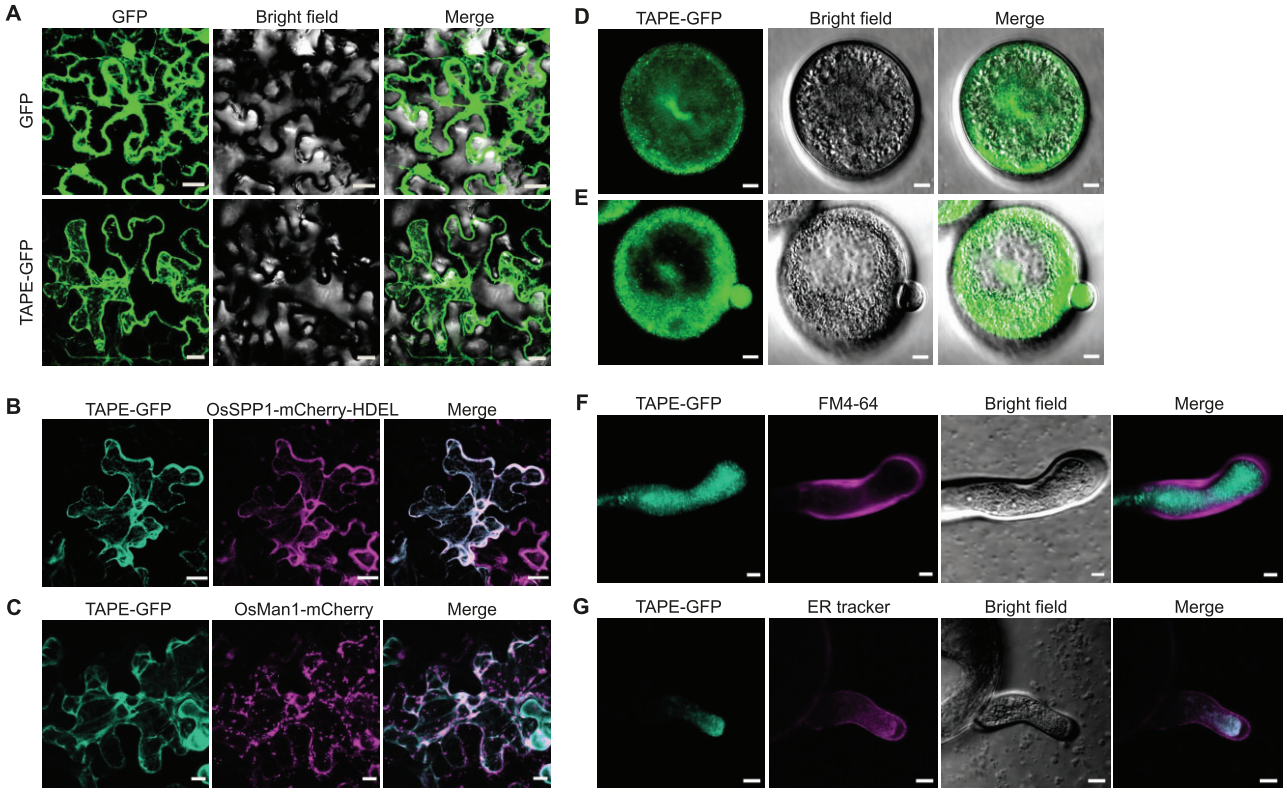

Figure 4 Subcellular localization of TAPE-GFP in *N. benthamiana* epidermal cells and rice PT. A, Subcellular localization of GFP and TAPE-GFP in *N. benthamiana* epidermal cell. The images were processed with the orthogonal projection method to check the in-depth subcellular localization of the TAPE-GFP. Bar = 20 μm. B–C, Co-localization of TAPE-GFP with the ER (B) and cis-Golgi (C) in *N. benthamiana* cells. The signal peptides from OsSPP1 and OsManI were fused with mCherry and used as ER and cis-Golgi marker proteins, respectively. The images were processed by orthogonal projection. Bar = 20 μm (B) and 10 μm (C). D–E, Subcellular localization of TAPE in PTs of the *pTAPE::TAPE-GFP* transgenic line (*TAPE-GFP* line). A representative pollen grain was photographed before (D) and after pollen germination (E) by confocal microscopy. Bar = 5 μm (D and E). F–G, Co-localization of the PM and ER in PTs of *TAPE-GFP* lines. The PTs were probed with FM4-64 (F) and ER-Tracker dyes (G). Bars = 2 μm and 5 μm, respectively.

tobacco (*Nicotiana benthamiana* L.) infiltration assay. In *N. benthamiana* epidermal cells, we observed that localization of the TAPE-GFP protein differed from GFP localized in the nucleus and cytosol (Figure 4A). TAPE-GFP was localized in a mesh structure all over the cells (Supplemental Movie S1), similar to the reported pattern of the ER in *N. benthamiana* cells (Cao et al., 2016). Using co-localization of TAPE-GFP with ER or cis-Golgi marker proteins, OsSPP1-mCherry-HDEL and OsManI-mCherry, respectively (Dangol et al., 2017), we found co-localization of TAPE-GFP with the ER marker

protein but not with a cis-Golgi marker (Figure 4, B and C; Supplemental Movies S2 and S3).

To verify and further characterize TAPE localization, we studied the subcellular localization of a C-terminal, GFP-fused transgenic line (*pTAPE::TAPE-GFP*; Figure 4, D–G). TAPE-GFP was localized evenly throughout the pollen grain (Figure 4D) and at growing PTs during germination (Figure 4E). In elongated PT, the TAPE-GFP did not colocalize with the plasma membrane (PM; Figure 4F) but colocalized with the ER at the subapical region of the PT (Figure 4G). These results confirmed that TAPE-GFP localized in the ER in both *N. benthamiana* epidermal cells and in the growing PT in rice, and it moved toward the tip of the PT when the pollen germinated.

TAPE encodes a myosin XI adaptor protein in rice

To obtain clues to the function of TAPE, we compared the amino acid sequence to its homologs in the Phytozome database (Supplemental Figure S3). We used homologs of TAPE with three TPR domains and a PB1 domain from 29 dicot and 13 monocot plants. Interestingly, these homologs were conserved in angiosperms, and they clustered according to the monocot and dicot classification. In this analysis, we found that *TAPE* is a putative ortholog of a myosin XI adaptor coding gene *MadB1* in Arabidopsis (Kurth et al., 2017). In addition, one of the maize (*Zea mays* L.) homologs, ZmHIP (GRMZM2G023275), interacted with OPAQUE1, a myosin XI in maize required for ER motility in the endosperm (Wang et al., 2012). These results suggested that TAPE might function as a myosin XI adaptor in rice. To confirm our hypothesis, we tested the binding between TAPE and the GTD of a myosin XI (LOC4330906) that is closely related to the maize OPAQUE1 in rice (Figure 5, A–D; Supplemental Figure S4A). Using a bait constructed with the C-terminal region of TAPE, we performed a Y2H assay (Figure 5A). The bait did not self-activate (Figure 5B) and interacted with a GTD of myosin XI upon selection (Figure 5C). To confirm this interaction, we performed bimolecular fluorescence complementation (BiFC) and co-immunoprecipitation (co-IP) assays (Supplemental Figure S4A; Figure 5D). Both experiments confirmed that TAPE was bound to myosin XI which is expressed in rice pollen (Supplemental Figure S4B).

In addition, we determined whether localization of TAPE-GFP depended on AF for TAPE to function as a myosin XI adaptor (Figure 5, E and F). Initially, we infiltrated the *N. benthamiana* leaf with TAPE-GFP and an AF marker, Lifeact-mCherry (Riedl et al., 2008), and treated the leaf with 10 nM of latrunculin B, an AF inhibitor (LatB). When LatB was added, the TAPE-GFP localization changed forming a small lump compared to the MOCK treatment (Figure 5E), and the dynamic movement of the TAPE with ER marker stopped with LatB (Supplemental Movie S4). TAPE localized differently in pollen grains and PT when it was treated with 2-nM LatB forming lumps (Figure 5F; Supplemental Figure S5). These results confirmed that *TAPE* is a gene encoding a myosin XI adaptor.

TAPE interacts with OsPLIM2b and EF1a

TPR and PB1 are well-known domains that mediate various protein-protein interactions (D'Andrea and Regan, 2003; Sumimoto et al., 2007). Therefore, we searched for interacting proteins of TAPE by Y2H screening using a yeast prey library with rice anther cDNAs (Figure 6; Supplemental Figure S6). When we constructed baits A and B, the GAL4 DNA binding domain fused to the TPR and PB1 domain, respectively, and Y2H screening (Figure 6A; Supplemental Figure S6A) identified five candidate proteins. We found one candidate protein for bait A (*Os04g54010* encoding LIM-domain containing protein, PLIM2b) and two proteins for bait B (*Os03g08050* encoding elongation factor 1 alpha, EF1a, and *Os10g40090* encoding expansinB9 [ExpB9]; Figure 6B; Supplemental Figure S6B). To confirm these interactors, we performed subcellular localization and BiFC assays (Supplemental Figure S7). OsPLIM2b and EF1a both showed co-localization and interaction with TAPE inside the *N. benthamiana* epidermal cells (Supplemental Figure S7, A and B), and those two interactions were confirmed by co-IP analysis indicating that TAPE interacts with OsPLIM2b and EF1a (Figure 6C). The RT-qPCR results of these two interactors support that these interactions could occur in rice pollen (Supplemental Figure S7C).

TAPE affects the transcription of genes related to cell organization, especially kinesin motors

Using anthers from the WT and *tape-1* strains we performed RNA-Seq analysis to understand the transcriptional regulation of *TAPE*. We identified 1,259 differentially expressed genes (DEGs), in the *tape-1* anther (799 were upregulated and 460 were downregulated) which were analyzed using the cell function overview in MapMan (Figure 7A). We found that genes for regulation, protein modification or degradation, and transport were differentially expressed in the *tape-1* anther. Notably, the cell organization gene category was substantially downregulated in the mutant anther. A Gene Ontology (GO) enrichment with the downregulated DEGs (Figure 7B) identified microtubule (MT)-based movement as the most enriched GO term. The GO term contains seven kinesin motor genes showing significant transcript reduction in the *tape-1* anther. We confirmed the reduction in expression for three kinesin motor-coding genes in the *tape-1* anther by RT-qPCR analysis (Figure 7C). These data suggest that *TAPE* is involved in the transcription of MT-related genes, especially kinesin motors.

Discussion

TAPE is an essential myosin XI adaptor for normal PT elongation in rice

PT elongation in rice is important for successful male gamete delivery and seed setting, which affects yield. In addition, the genes for PT elongation are a valuable genetic resource for the two-line hybrid system in the seed industry. Despite their importance, few genes have been characterized (Kim et al., 2019b). Here, we identified and characterized *TAPE*, which encodes a protein with three TPRs and a PB1 domain

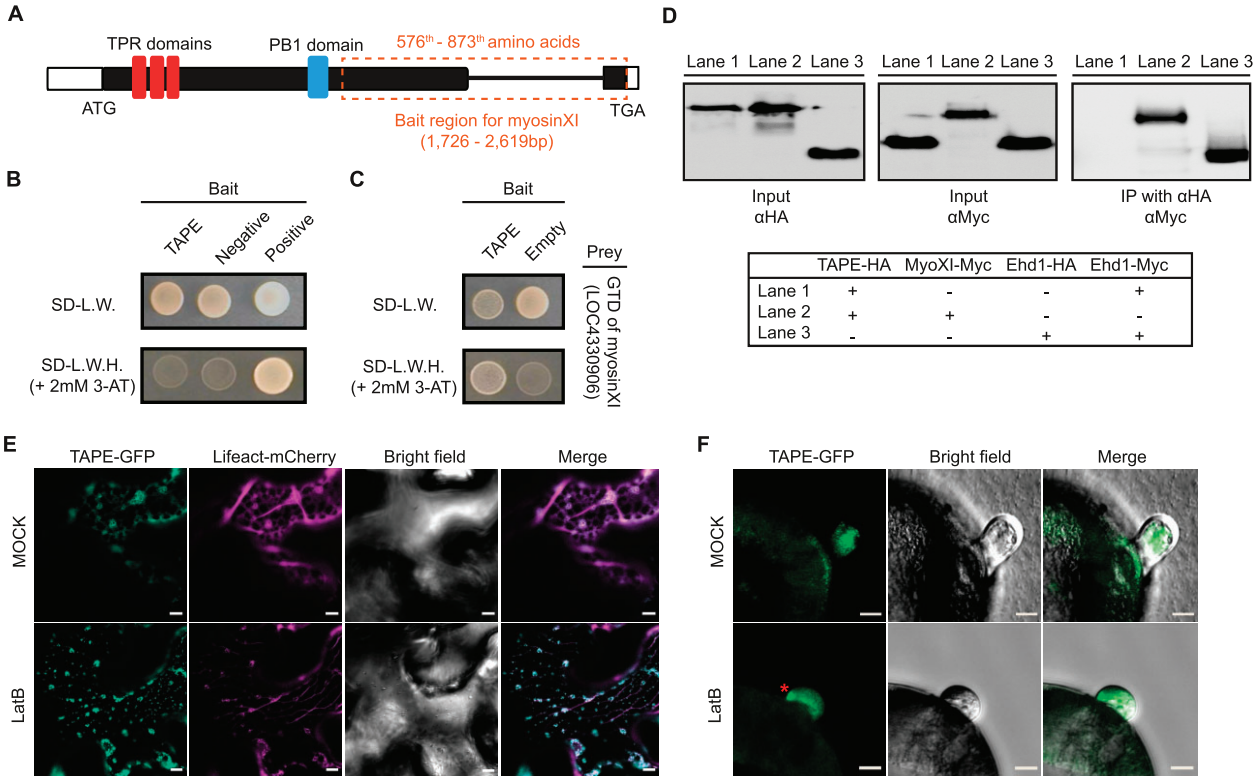

Figure 5 Myosin XI binding and AF-dependent localization of TAPE. A, Gene structure of *TAPE* and the bait region used for myosin XI binding assays. The orange dotted box indicates the bait region, corresponding to a homolog in maize (Wang et al., 2012). B, Y2H self-activation test for the TAPE bait encoding the GAL4 DNA binding domain fused to the C-terminal of TAPE. The bait vector contained murine p53 and prey vector with SV40 large T-antigen as a positive control. Empty vectors were the negative control. C, TAPE bound to the GTD of the myosin XI (LOC4330906) in the Y2H assay. D, co-IP of TAPE and myosin XI GTD. Ehd1-HA and Myc were the negative and positive controls, respectively. E–F, LatB treatment for AF-dependent localization of TAPE in *N. benthamiana* epidermal cells (E) and rice PT (F). *Nicotiana benthamiana* and pollen were treated with LatB at 10 nM and 2 nM, respectively, for an hour. The red asterisk in F indicates abnormally localized TAPE-GFP in the PT. Bar = 5 μm.

(Figure 1A) and is expressed in pollen after the bicellular pollen stage (Figure 3). We demonstrated by segregation experiments and reciprocal crossing using T-DNA lines that *TAPE* is a key player in male gamete transfer (Figure 1A; Table 1). HM KO mutants *tape-1* and *tape-2*, generated by CRISPR/Cas9, were sterile (Figure 1, B and C; Supplemental Figure S1, A and B). The *tape-1* strain had PTs that were short but intact and ruptured normally after elongation (Figure 2) and had normal germination compared to the WT (Supplemental Figure S2). Thus, *TAPE* is responsible for PT elongation in rice. Comparison of TAPE with other proteins revealed it to be a myosin XI adaptor protein (Supplemental Figure S3) which was confirmed by its interaction with the GTD of pollen-expressed myosin XI in protein-binding assays (Figure 5, C and D; Supplemental Figure S4). Together, our data indicate that TAPE is a key myosin XI adaptor that is required for normal PT elongation in rice.

TAPE is a possible mediator of actomyosin-driven transport of organelles and proteins in rice PT elongation

TAPE was mainly localized to the ER in both *N. benthamiana* epidermal cells and rice PT (Figure 4, B and G), consistent with a previous report for ZmHIP, a TAPE-homolog in maize (Wang et al., 2012). ZmHIP binds to the myosin XI OPAQUE1 and is involved in ER motility in the maize endosperm. By Y2H screening we identified interactions between TAPE and OsPLIM2b and EF1a that are expressed in rice pollen (Figure 6; Supplemental Figure S7). LatB treatment showing AF-dependent movement of TAPE (Figure 5, E and F; Supplemental Figure S5; Supplemental Movies S2 and S4) and co-localization assays of TAPE with its interactors and an ER marker (Supplemental Movies S5 and S6) indicate that TAPE might mediate the actomyosin-dependent transport of the ER and the interactors in rice PT elongation.

The interaction of plant organelles with membrane contact sites is important in organelle motility (Perico and Sparkes, 2018). Consistently, we observed similar dynamics in *N. benthamiana* cells between TAPE and the cis-Golgi marker in our co-localization assay (Figure 4C; Supplemental Movie S3). In Arabidopsis, *MadB1*, also known as *AtPhox1* (Prasad et al., 2010), and a putative ortholog of *TAPE* (Supplemental Figure S3), encodes a carboxylate clamp-type TPR protein and a co-chaperone of heat shock protein 70 (Hsp70) and Hsp90. *MadB2*, which is a paralog of *MadB1* in Arabidopsis, is also known as *CLUMPED CHLOROPLAST1* (*CLMP1*), and a KO

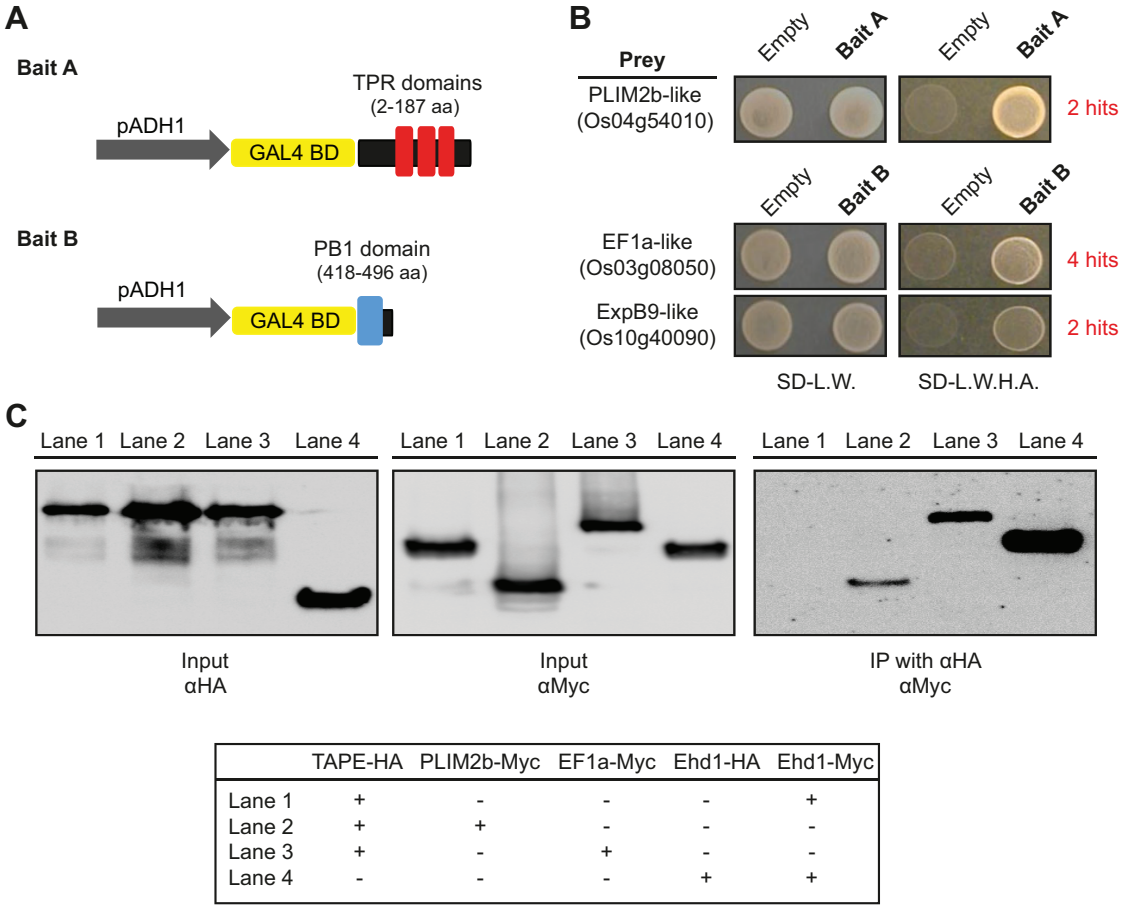

	TAPE-HA	PLIM2b-Myc	EF1a-Myc	Ehd1-HA	Ehd1-Myc
Lane 1	+	-	-	-	+
Lane 2	+	+	-	-	-
Lane 3	+	-	+	-	-
Lane 4	-	-	-	+	+

Figure 6 Identification of interaction partners of the TAPE protein. A, Diagrams of two bait vectors for Y2H screening. BD, DNA binding domain of yeast GAL4 transcription factor. B, Partners interacting with TAPE by Y2H. Empty, an empty bait vector used as a negative control. Hits, the number of times the interaction occurred in the Y2H screening. C, co-IP of TAPE with proteins OsPLIM2b and EF1a.

clmp1-1 mutant showed abnormal plastid distribution in various organs (Yang et al., 2011). How TAPE can localize to the ER without a transmembrane domain remains to be determined; however, these results suggest that TAPE might mediate the actomyosin-dependent transport of various organelles and proteins during PT elongation in rice.

TAPE is involved in the transcriptional regulatory network in rice PT elongation

Transcriptome analysis of *tape-1* versus WT anthers revealed that *TAPE* affects transcriptional regulation for various biological functions, especially cell organization (Figure 7A). Paradoxically, the absence of *TAPE* affected the transcription of MT-related motors, such as kinesins, even though TAPE is a myosin XI adaptor for the AF-related motor (Figure 7, B and C). Further research will be needed to determine whether there is a transcriptional connection between the two cytoskeletons, AF and MT, in addition to the physical connection previously reported (Schneider and Persson, 2015).

Conclusion

In this study, we report that *TAPE* encodes an essential myosin XI adaptor associated with the actomyosin-dependent movement in rice PT elongation, and we provide a model for the role of *TAPE* in the rice PT elongation process (Figure 8). The functional characterization of a myosin XI adaptor, TAPE will improve our understanding of myosin XI-mediated transport in plants and the PT elongation process in rice.

Materials and methods

Plant materials and growth conditions

WT rice (*O. sativa* spp. Japonica cv. Dongin and Hwayoung) and transgenic lines were grown in a growth chamber under the following conditions: 28°C/25°C (day/night), 16/8 h (light/dark), and 80% humidity for 2 weeks and transferred to the paddy field located at Kyung Hee University in Yongin, Republic of Korea, from May 2018 to October 2020. The T-DNA mutant of *TAPE* (2B-00091; cv. Hwayoung), was obtained from the seed bank in the Kyung Hee University (Yi and An, 2013). We used the heterozygous (HZ) mutant for the segregation analysis and reciprocal crossing. The seeds were grown on Murashige and Skoog media for 2 weeks in a CO_2 incubator and transferred to the growth chamber. *Nicotiana benthamiana* plants for the agro-infiltration assay were grown in a growth chamber at 25°C, in 12/12 h (light/dark) and 60% humidity for 3 weeks.

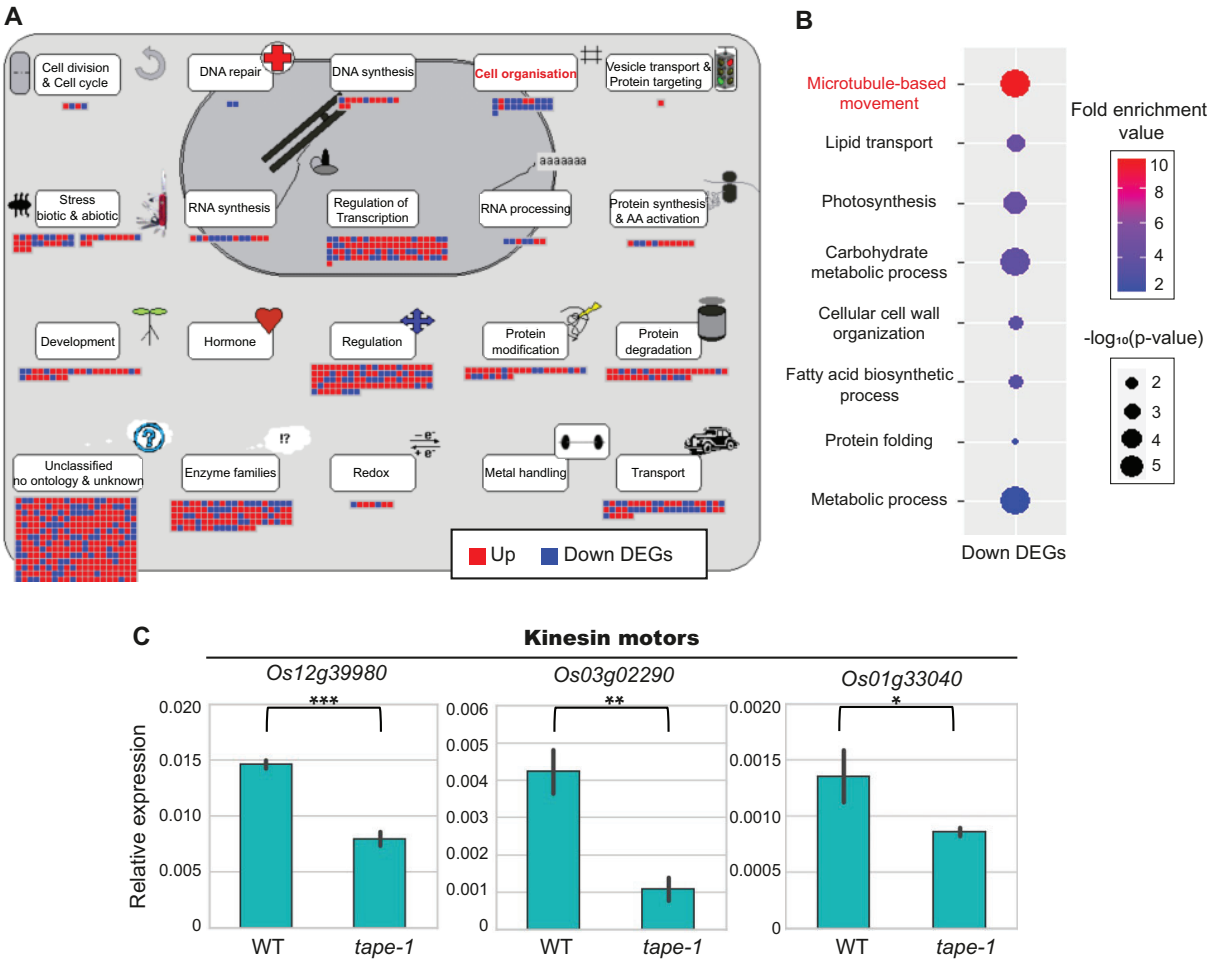

Figure 7 Transcriptome analysis of the *tape-1* anther. A–B, Functional classification of DEGs in the *tape-1* anther compared to the WT anther. A, Cell function overview in the MapMan program. The red and blue squares indicate upregulated and downregulated DEGs in *tape-1*, respectively. The cell organization category is highlighted with red letters. B, A Gene Ontology (GO) enrichment analysis of the downregulated DEGs to identify GO terms related to cell organization. Only GO terms with more than five query numbers were used. The size and color of the dots indicate the statistical significance and enrichment value for each GO term. C, Expression of genes for MT motors in *tape-1* anther. Relative expression was determined by RT-qPCR and calculated as $2^{-\Delta\Delta Ct}$ with normalization to *OsUbi5*. Bars indicate the mean values of the three replicates with their standard deviations. *P*-values from the Student's t test are indicated as follow: $^{*}P < 0.05$, $^{**}P < 0.01$, and $^{***}P < 0.001$.

Vector cloning and tissue culture

Guide RNAs (gRNAs) to generate two KO mutants (*tape-1* and *tape-2*) of *TAPE* were designed using CRISPRdirect and CAFRI-Rice web software (Naito et al., 2015; Hong et al., 2020). Oligomers corresponding to the gRNAs were annealed and ligated into the BsaI-treated pRGEB32 binary vector (Addgene plasmid number: 63142).

To generate the *TAPE* promoter-driven GFP (*pTAPE*::*TAPE-GFP*), and GUS fusion transgenic lines (*pTAPE*::*TAPE-GUS*), a 1,233-bp promoter with the 2,523-bp coding sequence (CDS), except for stop codon, of *TAPE* was amplified. The amplicon was ligated into the BamHI-treated pGA3519 binary vector and the BamHI and HindIII-treated pGA3427 binary vector for C-terminal (C-term) GUS and GFP fusions, respectively, using the In-Fusion HD Cloning Kit (639648; Takara, Shiga, Japan). The constructs were transformed into *Agrobacterium tumefaciens* LBA4404 for stable transformation by Agrobacterium-mediated co-cultivation (Lee et al., 1999).

The CDSs of *TAPE* and its interactors (*OsPLIM2b*, *Os04g45010*; *EF1a*, *Os03g08050*; *OsExpB9*, and *Os10g40090*) were amplified to generate p35S driven C-term GFP (*p35S*::*TAPE-GFP*) and mRFP-fused constructs (*p35S*::interactors-*mRFP*). The amplicons were cloned into HindIII-digested vectors. For the BiFC assay, the amplified CDSs were ligated into the HindIII-digested p35S driven N- (NV) or C-term Venus (CV) binary vectors. The primers used in cloning are listed in Supplemental Table S1.

Plant phenotyping and pollen germination analysis

The WT and *tape-1* plants were photographed before harvesting using a COOLPIX P900s camera (Nikon, Tokyo, Japan), and the spikelets from those plants at the anthesis

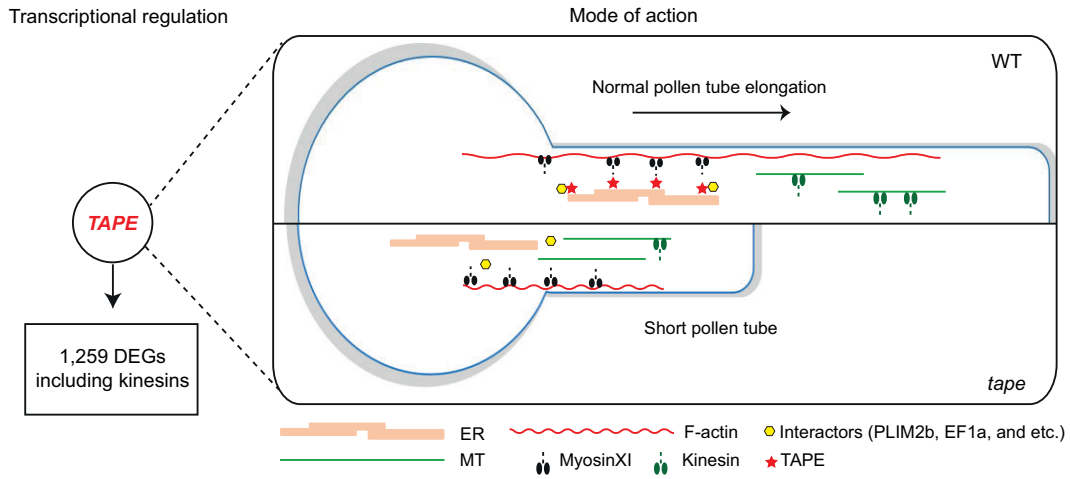

Figure 8 Model for *TAPE* functions in rice PT elongation. *TAPE* transcriptionally regulates 1,259 DEGs, especially MT-movement associate motors, kinesins. TAPE is a myosin XI adaptor protein that is localized to the ER where it mediates actomyosin-based transport by binding with interactors such as OsPLIM2b and EF1a in rice PT elongation. In the *tape* KO mutant, actomyosin movement of the ER and interactors is disrupted so that the PT cannot elongate sufficiently for fertilization to occur.

stage were collected and imaged using a SZX61 microscope (Olympus, Tokyo, Japan).

To observe pollen morphology, the pollen grains were collected by tweezing the anther and were stained for starch content, and inner and outer cell wall layers. Briefly, a 1% w/v I_2-KI solution was used to stain starch and 0.1% calcofluor white and 0.001% auramine O solutions were used to stain intine and exine layers, respectively. The stained pollens were observed using a BX61 microscope (Olympus, Tokyo, Japan) with brightfield, ultra-violet (UV), and fluorescein isothiocyanate channels.

For pollen germination analysis, released pollen grains from the dehiscent anther were collected on a solid or liquid pollen germination medium as previously described (Kim et al., 2020). PT length and pollen germination ratio were measured for at least 150 pollen grains using the ImageJ software. To observe PT elongation in the pistil, we stained the pistil with aniline blue solution as described by Liu et al., (2016) with some modifications. The pistils were collected 2 h after pollination and incubated in Carnoy's solution overnight. The fixed pistils were washed 5 times with distilled water (DW), incubated in 1 M NaOH solution for 6 h until they became transparent, washed twice with DW, and stained with 0.05% aniline blue (in 0.1 M K2HPO4, pH 8.5 solution) for 1 h in the dark. The stained pistils were observed under the UV channel.

Nucleic acid extraction and RT-qPCR analysis

Genomic DNA, extracted from the leaf sample with cetyltrimethylammonium bromide, was used for genotyping T-DNA mutants and sequencing CRISPR/cas9 mutants. For RNA extraction, various tissue samples as described previously (Moon et al., 2019) were immediately frozen with liquid N_2. The pollen grains were stabilized with RNAlater (Invitrogen, Waltham, MA, USA) after collecting fresh samples from dehiscent anthers in the paddy field. Total RNA was extracted according to the manufacturer's instructions for RNeasy Plant Mini Kit (Qiagen, Hilden, Germany). Complementary DNA (cDNA) was synthesized from RNA using a SuPrimeScript RT premix kit (GeNet Bio, Daejeon, South Korea) with a 1-h incubation at 50°C.

RT-qPCR analysis was performed with the Roter-Gene Q system (Qiagen, Hilden, Germany) and 2X Prime Q-Mastermix (GeNet Bio). Expression was normalized to the rice ubiquitin 5 gene (*OsUbi5*, *Os01g22490*) as previously described (Moon et al., 2020) and the $2^{-\Delta\Delta Ct}$ method was used to calculate relative expression (Schmittgen and Livak, 2008). The primers for RT-qPCR analysis are listed in Supplemental Table S1.

Histochemical GUS assay

Spikelets of the GUS fusion transgenic line (*pTAPE::TAPE-GUS*) at different developmental stages and pollen grains were stained with GUS solution for 2 h at 37°C. The stained spikelet and pollen grains were imaged using the SZX61 microscope.

Subcellular localization analysis

For subcellular localization analysis in *N. benthamiana* epidermal cells, the cloned p35S-driven constructs were transformed into *A. tumefaciens* GV3101 using the freeze-thaw method and transformed GV3101 were infiltrated into *N. benthamiana* leaves using a *N. benthamiana* infiltration assay as previously reported (Sparkes et al., 2006). After 72 h of infiltration, leaves were observed using an LSM 510 META confocal scanning laser microscope (CSLM; Carl Zeiss, Jena, Germany). GFP and RFP fluorescence was observed under 488/505–530 and 543/560–615 nm filters (excitation/emission wavelength), respectively. Images were analyzed and exported using Zeiss ZEN lite software.

The subcellular localization of TAPE in the PT of the *pTAPE::TAPE-GFP* plant was also imaged using CSLM. To

visualize the PM and ER, the elongated PTs were stained with 10 μM FM4-64 (T13320; Invitrogen, Waltham, MA, USA) and 1 μM ER-Tracker Red dye (E34250; Invitrogen, Waltham, MA, USA). To determine the AF-dependent movement of TAPE, 2 nM or 10 nM LatB was added to the infiltrated leaves and PT, respectively.

Phylogenetic analysis

TAPE was compared to the protein sequences of its homologs in angiosperm for 29 dicots and 13 monocots that were retrieved from the Phytozome database (Goodstein et al., 2012). The most similar protein homologs with a similarity score of over 1,000 were selected for each species. The sequences were aligned with the MUSCLE program and a phylogenetic tree based on a neighbor-joining method with 1,000 bootstrapping was created using MEGA X software (Kumar et al., 2018). The information of the homologs is listed in Supplemental Table S2.

Y2H assays

The 4–561-bp, 1,252–1,488-bp, and 1,726–2,619-bp fragments of the *TAPE* CDS were amplified and cloned into the EcoRI/BamHI-digested pGBKT7 vector to generate GAL4 DNA binding domain fused bait (bait A, B, and C respectively). The constructs were transformed into the yeast AH109 for the self-activation test. These yeast transformants did not grow on a minimal synthetic defined (SD) medium and showed no transcriptional activation. Bait A and B were used for the Y2H screening assay, performed by Panbionet Corp (Pohang, Republic of Korea; www.panbionet.com) with the same rice anther cDNA library used in our previous study (Kim et al., 2021a).

To determine whether TAPE bound myosin XI, a Y2H assay was performed using bait C. The GTD of myosin XI (LOC4330906) was fused with the GAL4 activation domain. SD medium lacking Leu, Trp, and His was the selection media with 5 mM 3-amino-1,2,4-triazole (3-AT).

co-IP assays

For constructing the Myc or HA fusions, *TAPE*, *myosin XI*, *OsPLIM2b*, and *EF1a* full-length cDNAs without the stop codons were inserted into pGA3817 with the 6X-Myc coding region or into pGA3818 with 3X-HA. The fusion molecules were transformed into Oc cell protoplasts by polyethylene glycol transformation. After incubation for 12–14 h at 28°C, the protoplasts were isolated and used for co-IP assays, as previously described (Cho et al., 2016; Yoon et al., 2017). Before the protoplasts were harvested, anti-HA mouse monoclonal antibodies (12CA5; Roche, Mannheim, Germany, http://www.roche.com) were incubated for 3 h with Protein A/G agarose beads (Millipore, Billerica, MA, USA; http://www.emdmillipore.com) in a binding buffer [75 mM NaCl, 50 mM Tris–HCl (pH 7.5), 5 mM EDTA, 1 mM dithiothreitol, 1 mM phenylmethanesulfonylfluoride, and 1% Triton X-100]. Then the protoplasts were isolated and resuspended in an IP buffer [75 mM NaCl, 50 mM Tris–HCl (pH 7.5), 5 mM EDTA, 1% Triton X-100, 1 mM dithiothreitol, 1 mM phenylmethanesulfonylfluoride, 2 mM NaF, 100 μM MG132, and protease inhibitor cocktail (Roche, Basel, Switzerland)]. Pre-cleared samples were incubated for 6 h with the anti-HA mouse monoclonal antibodies that were bound with the Protein A/G-conjugated agarose beads. After washing with a buffer [75 mM KCl, 50 mM Tris–HCl (pH 7.5), 5 mM EDTA, 0.1% Triton X-100, 1 mM dithiothreitol, and 1 mM phenylmethanesulfonylfluoride], the bound proteins were eluted with IP buffer and a protein loading dye. The eluted proteins were resolved by 10% SDS-PAGE and transferred to a polyvinylidene difluoride membrane (Millipore, Burlington, MA, USA). The blotting membrane was incubated in a blocking solution with HRP-conjugated anti-Myc monoclonal antibodies (#2040; Cell Signaling, Beverly, MA, USA). Proteins bound to the membrane were detected using an enhanced chemiluminescence prime western blotting detection reagent (WSE-7120S; ATTO, Tokyo, Japan; https://www.atto.co.jp/) with the ChemiDoc MP Imaging System (17001402; Biorad, Hercules, USA). Primers for full-length amplifications are listed in Supplemental Table S1.

Transcriptome analysis

Mature pollen grains containing anthers at stages 13–14 (Zhang et al., 2011) were used for RNA-Seq analysis. After the sample quality control process, a sequencing library was constructed using TruSeq Stranded mRNA LT Sample Prep Kit (Illumina, San Diego, CA, USA) following the manufacturer's instruction (Part #15031047 Rev. E). The library was sequenced using the Illumina NovaSeq 6000 platform at MacroGen Inc with FASTQ formatted raw data files.

The raw files were trimmed using the Cutadapt program (Martin, 2011) with parameters: -a AGATCGGAAGAGC -A AGATCGGAAGAGC -q 30 -m 20 and the reads were mapped to a rice reference genome from the rice genome annotation project (RGAP; http://rice.plantbiology.msu.edu/) using HISAT2 aligner with default parameters (Kim et al., 2019a). The raw reads were counted using the featureCounts program (Liao et al., 2014) and the DEG analysis was performed with the DESeq2 R package (Love et al., 2014). The DEGs were selected based on these criteria: p and adjusted P-value < 0.05, and $|\log2(\text{fold change})| \geqslant 1$. GO enrichment and MapMan analyses of the DEGs were performed as previously described (Shin et al., 2020). Among enriched GO terms, we adopted the terms with a query number over five for reliable terms.

Statistical analyses

For statistical analysis on PT length and pollen germination rate, >150 pollen grains of the WT and *tape-1* plants were counted. Student's t test was performed using T.TEST() function embedded in EXCEL software.

Accession numbers

The locus and sequence information for *TAPE* were retrieved from the RGAP database (*TAPE*: *Os09g03890*). The raw data were deposited at the ArrayExpress (https://www.ebi.ac.uk/arrayexpress/) with the accession number E-MTAB-10439.

Supplemental data

The following materials are available in the online version of this article.

Supplemental Figure S1. Phenotype of the *tape-2* mutant.

Supplemental Figure S2. Germination ratio of the WT plant and *tape-1*.

Supplemental Figure S3. Comparative analysis of TAPE and its homologs in angiosperms.

Supplemental Figure S4. BiFC analysis of TAPE with the C-terminal GTD of myosin XI and expression analysis of the myosin XI gene.

Supplemental Figure S5. A 2 nM LatB treatment disturbs the subcellular localization of TAPE in the pollen grain and PT.

Supplemental Figure S6. Self-activation test of the baits used in Y2H assay.

Supplemental Figure S7. Co-localization and BiFC assays of TAPE with its interactors and expression analysis of genes encoding the interactors.

Supplemental Table S1. Primers used in this study.

Supplemental Table S2. Information on the TAPE homologs used in comparative studies.

Supplemental Movie S1. Z-stack images of TAPE-GFP in *N. benthamiana* epidermal cells.

Supplemental Movie S2. Time-series images of TAPE-GFP and OsSPP1-mCherry-HDEL in *N. benthamiana* epidermal cells.

Supplemental Movie S3. Time-series images of TAPE-GFP and OsManI-mCherry in *N. benthamiana* epidermal cells.

Supplemental Movie S4. Time-series images of TAPE-GFP and OsSPP1-mCherry-HDEL in *N. benthamiana* epidermal cells with 10 nM LatB treatment.

Supplemental Movie S5. Time-series images of TAPE-NV and PLIM2b-CV with OsSPP1-mCherry-HDEL in *N. benthamiana* epidermal cells.

Supplemental Movie S6. Time-series images of TAPE-NV and EF1a-CV with OsSPP1-mCherry-HDEL in *N. benthamiana* epidermal cells.

Acknowledgments

We thank Prof. Gynheung An (Kyung Hee University) for providing valuable comments.

Funding

This work was supported by grants from the New Breeding Technologies Development Program (PJ01661002 to K.-H.J.), the Rural Development Administration, Republic of Korea, and grants by the National Research Foundation, Ministry of Education, Science and Technology (2021M3E5E6025387 to K.-H.J., 2021R1C1C2091377 to W.-J.H., 2019R1C1C1002636 to Y.-J.K., and 2021R1A4A2001968 to S.T.K.).

Conflict of interest statement. None declared.

References

Avisar D, Abu-Abied M, Belausov E, Sadot E, Hawes C, Sparkes IA (2009) A comparative study of the involvement of 17 Arabidopsis myosin family members on the motility of golgi and other organelles. Plant Physiol **150**: 700–709

Cai G, Cresti M (2009) Organelle motility in the pollen tube: a tale of 20 years. J Exp Bot **60**: 495–508

Cao P, Renna L, Stefano G, Brandizzi F (2016) SYP73 anchors the ER to the actin cytoskeleton for maintenance of ER integrity and streaming in Arabidopsis. Curr Biol **26**: 3245–3254

Chandran AKN, Hong WJ, Abhijith B, Lee J, Kim YJ, Park SK, Jung KH (2020) Rice male gamete expression database (RMEDB): a web resource for functional genomic studies of rice male organ development. J Plant Biol **63**: 421–430

Chen LQ, Ye D (2007) Roles of pectin methylesterases in pollen-tube growth. J Integr Plant Biol **49**: 94–98

Cho LH, Yoon J, Pasriga R, An G (2016) Homodimerization of Ehd1 is required to induce flowering in rice. Plant Physiol **170**: 2159–2171

D'Andrea LD, Regan L (2003) TPR proteins: the versatile helix. Trends Biochem Sci **28**: 655–662

Dangol S, Singh R, Chen Y, Jwa NS (2017) Visualization of multicolored in vivo organelle markers for co-localization studies in *Oryza sativa*. Mol Cells **40**: 828–836

Feng H, Liu C, Fu R, Zhang M, Li H, Shen L, Wei Q, Sun X, Xu L, Ni B, et al. (2019) LORELEI-LIKE GPI-ANCHORED PROTEINS 2/3 regulate pollen tube growth as chaperones and coreceptors for ANXUR/BUPS receptor kinases in Arabidopsis. Mol Plant **12**: 1612–1623

Goodstein DM, Shu S, Howson R, Neupane R, Hayes RD, Fazo J, Mitros T, Dirks W, Hellsten U, Putnam N, et al. (2012) Phytozome: a comparative platform for green plant genomics. Nucleic Acids Res **40**: D1178–D1186

Gu Y, Vernoud V, Fu Y, Yang Z (2003) ROP GTPase regulation of pollen tube growth through the dynamics of tip-localized F-actin. J Exp Bot **54**: 93–101

Hoffmann RD, Portes MT, Olsen LI, Damineli DSC, Hayashi M, Nunes CO, Pedersen JT, Lima PT, Campos C, Feijó JA, et al. (2020) Plasma membrane H + -ATPases sustain pollen tube growth and fertilization. Nat Commun **11**: 2395

Hong WJ, Kim YJ, Kim EJ, Chandran AKN, Moon S, Gho YS, Yoou MH, Kim ST, Jung KH (2020) CAFRI-Rice: CRISPR applicable functional redundancy inspector to accelerate functional genomics in rice. Plant J **104**: 532–545

Jiang S, Ramachandran S (2004) Identification and molecular characterization of myosin gene family in *Oryza sativa* genome. Plant Cell Physiol **45**: 590–599

Johnson MA, Harper JF, Palanivelu R (2019) A fruitful journey: pollen tube navigation from germination to fertilization. Annu Rev Plant Biol **70**: 809–837

Kim D, Paggi JM, Park C, Bennett C, Salzberg SL (2019a) Graph-based genome alignment and genotyping with HISAT2 and HISAT-genotype. Nat Biotech **37**: 907–915

Kim EJ, Park SW, Hong WJ, Silva J, Liang W, Zhang D, Jung KH, Kim YJ (2020) Genome-wide analysis of RopGEF gene family to identify genes contributing to pollen tube growth in rice (*Oryza sativa*). BMC Plant Biol **20**: 95

Kim YJ, Kim MH, Hong WJ, Moon S, Kim EJ, Silva J, Lee J, Lee S, Kim ST, Park SK, et al. (2021a) GORI, encoding the WD40 domain protein, is required for pollen tube germination and elongation in rice. Plant J **105**: 1645–1664

Kim YJ, Kim MH, Hong WJ, Moon S, Kim ST, Park SK, Jung KH (2021b) OsMTD2-mediated reactive oxygen species (ROS) balance is essential for intact pollen-tube elongation in rice. Plant J **107**: 1131–1147

Kim YJ, Zhang D, Jung KH (2019b) Molecular basis of pollen germination in cereals. Trends Plant Sci **24**: 1126–1136

Kroeger J, Geitmann A (2012) The pollen tube paradigm revisited. Curr Opin Plant Biol **15**: 618–624

Kumar S, Stecher G, Li M, Knyaz C, Tamura K (2018) MEGA X: molecular evolutionary genetics analysis across computing platforms. Mol Biol Evol **35**: 1547–1549

Kurth EG, Peremyslov VV, Turner HL, Makarova KS, Iranzo J, Mekhedov SL, Koonin EV, Dolja VV (2017) Myosin-driven transport network in plants. Proc Natl Acad Sci USA **114**: E1385–E1394

Lee S, Jeon JS, Jung KH, An G (1999) Binary vectors for efficient transformation of rice. J Plant Biol **42**: 310

Lee SK, Hong WJ, Silva J, Kim EJ, Park SK, Jung KH, Kim YJ (2021) Global identification of ANTH genes involved in rice pollen germination and functional characterization of a key member, OsANTH3. Front Plant Sci **12**: 609473 doi: 10.3389/fpls.2021.609473

Li H, Lin Y, Heath RM, Zhu MX, Yang Z (1999) Control of pollen tube tip growth by a rop GTPase–dependent pathway that leads to tip-localized calcium influx. Plant Cell **11**: 1731–1742

Liao Y, Smyth GK, Shi W (2014) featureCounts: an efficient general purpose program for assigning sequence reads to genomic features. Bioinformatics **30**: 923–930

Liu L, Zheng C, Kuang B, Wei L, Yan L, Wang T (2016) Receptor-like kinase RUPO interacts with potassium transporters to regulate pollen tube growth and integrity in rice. PLoS Genet **12**: e1006085

Love MI, Huber W, Anders S (2014) Moderated estimation of fold change and dispersion for RNA-seq data with DESeq2. Genome Biol **15**: 550

Madison SL, Buchanan ML, Glass JD, McClain TF, Park E, Nebenführ A (2015) Class XI myosins move specific organelles in pollen tubes and are required for normal fertility and pollen tube growth in Arabidopsis. Plant Physiol **169**: 1946–1960

Martin M (2011) Cutadapt removes adapter sequences from high-throughput sequencing reads. EMBnet J **17**: 10–12

Mecchia MA, Santos-Fernandez G, Duss NN, Somoza SC, Boisson-Dernier A, Gagliardini V, Martínez-Bernardini A, Fabrice TN, Ringli C, Muschietti JP, et al. (2017) RALF4/19 peptides interact with LRX proteins to control pollen tube growth in Arabidopsis. Science **358**: 1600–1603

Michard E, Simon AA, Tavares B, Wudick MM, Feijó JA (2017) Signaling with ions: the keystone for apical cell growth and morphogenesis in pollen tubes. Plant Physiol **173**: 91–111

Moon S, Chandran AKN, Kim YJ, Gho Y, Hong WJ, An G, Lee C, Jung KH (2019) Rice RHC encoding a putative cellulase is essential for normal root hair elongation. J Plant Biol **62**: 82–91

Moon S, Hong WJ, Kim YJ, Chandran AKN, Gho YS, Yoo YH, Nguyen VNT, An G, Park SK, Jung KH (2020) Comparative transcriptome analysis reveals gene regulatory mechanism of UDT1 on anther development. J Plant Biol **63**: 289–296

Moon S, Jung KH (2020) First steps in the successful fertilization of rice and Arabidopsis: pollen longevity, adhesion and hydration. Plants **9**: 956

Moon S, Oo MM, Kim B, Koh HJ, Oh SA, Yi G, An G, Park SK, Jung KH (2018) Genome-wide analyses of late pollen-preferred genes conserved in various rice cultivars and functional identification of a gene involved in the key processes of late pollen development. Rice **11**: 28

Naito Y, Hino K, Bono H, Ui-Tei K (2015) CRISPRdirect: software for designing CRISPR/Cas guide RNA with reduced off-target sites. Bioinformatics **31**: 1120–1123

Peremyslov VV, Morgun EA, Kurth EG, Makarova KS, Koonin EV, Dolja VV (2013) Identification of myosin XI receptors in Arabidopsis defines a distinct class of transport vesicles. Plant Cell **25**: 3022–3038

Perico C, Sparkes I (2018) Plant organelle dynamics: cytoskeletal control and membrane contact sites. New Phytol **220**: 381–394

Prasad BD, Goel S, Krishna P (2010) In silico identification of carboxylate clamp type tetratricopeptide repeat proteins in Arabidopsis and rice as putative co-chaperones of Hsp90/Hsp70. PLoS One **5**: e12761

Riedl J, Crevenna AH, Kessenbrock K, Yu JH, Neukirchen D, Bista M, Bradke F, Jenne D, Holak TA, Werb Z, et al. (2008) Lifeact: a versatile marker to visualize F-actin. Nat Methods **5**: 605–607

Ross JL, Ali MY, Warshaw DM (2008) Cargo transport: molecular motors navigate a complex cytoskeleton. Curr Opin Cell Biol **20**: 41–47

Schmittgen TD, Livak KJ (2008) Analyzing real-time PCR data by the comparative CT method. Nat Protoc **3**: 1101–1108

Schneider R, Persson S (2015) Connecting two arrays: the emerging role of actin-microtubule cross-linking motor proteins. Front Plant Sci **6**: 415 doi: 10.3389/fpls.2015.00415

Shin NH, Trang DT, Hong WJ, Kang K, Chuluuntsetseg J, Moon JK, Yoo YH, Jung KH, Yoo SC (2020) Rice senescence-induced receptor-like kinase (OsSRLK) is involved in phytohormone-mediated chlorophyll degradation. Int J Mol Sci **21**: 260

Sparkes IA, Runions J, Kearns A, Hawes C (2006) Rapid, transient expression of fluorescent fusion proteins in tobacco plants and generation of stably transformed plants. Nat Protoc **1**: 2019–2025

Stephan O, Cottier S, Fahlén S, Montes-Rodriguez A, Sun J, Eklund DM, Klahre U, Kost B (2014) RISAP is a TGN-associated RAC5 effector regulating membrane traffic during polar cell growth in tobacco. Plant Cell **26**: 4426–4447

Sumimoto H, Kamakura S, Ito T (2007) Structure and function of the PB1 domain, a protein interaction module conserved in animals, fungi, amoebas, and plants. Sci STKE **2007**: re6–re6

Tamura K, Iwabuchi K, Fukao Y, Kondo M, Okamoto K, Ueda H, Nishimura M, Hara-Nishimura I (2013) Myosin XI-i links the nuclear membrane to the cytoskeleton to control nuclear movement and shape in Arabidopsis. Curr Biol **23**: 1776–1781

Tominaga M, Ito K (2015) The molecular mechanism and physiological role of cytoplasmic streaming. Curr Opin Plant Biol **27**: 104–110

Tominaga M, Kojima H, Yokota E, Orii H, Nakamori R, Katayama E, Anson M, Shimmen T, Oiwa K (2003) Higher plant myosin XI moves processively on actin with 35 nm steps at high velocity. EMBO J **22**: 1263–1272

Tominaga M, Nakano A (2012) Plant-specific myosin XI, a molecular perspective. Front Plant Sci **3**: 211 doi: 10.3389/fpls.2012.00211

Ueda H, Tamura K, Hara-Nishimura I (2015) Functions of plant-specific myosin XI: from intracellular motility to plant postures. Curr Opin Plant Biol **28**: 30–38

Ueda H, Yokota E, Kutsuna N, Shimada T, Tamura K, Shimmen T, Hasezawa S, Dolja VV, Hara-Nishimura I (2010) Myosin-dependent endoplasmic reticulum motility and F-actin organization in plant cells. Proc Natl Acad Sci USA **107**: 6894–6899

Vogler H, Santos-Fernandez G, Mecchia MA, Grossniklaus U (2019) To preserve or to destroy, that is the question: the role of the cell wall integrity pathway in pollen tube growth. Curr Opin Plant Biol **52**: 131–139

Wang G, Wang F, Wang G, Wang F, Zhang X, Zhong M, Zhang J, Lin D, Tang Y, Xu Z, et al. (2012) Opaque1 encodes a myosin XI motor protein that is required for endoplasmic reticulum motility and protein body formation in maize endosperm. Plant Cell **24**: 3447–3462

Wang X, Sheng X, Tian X, Zhang Y, Li Y (2020) Organelle movement and apical accumulation of secretory vesicles in pollen tubes of *Arabidopsis thaliana* depend on class XI myosins. Plant J **104**: 1685–1697

Xu Y, Huang S (2020) Control of the actin cytoskeleton within apical and subapical regions of pollen tubes. Front Cell Dev Biol **8**: 614821 doi: 10.3389/fcell.2020.614821

Yang Y, Sage TL, Liu Y, Ahmad TR, Marshall WF, Shiu SH, Froehlich JE, Imre KM, Osteryoung KW (2011) CLUMPED CHLOROPLASTS 1 is required for plastid separation in Arabidopsis. Proc Natl Acad Sci USA **108**: 18530–18535

Yi J, An G (2013) Utilization of T-DNA tagging lines in rice. J Plant Biol **56**: 85–90

Yoon J, Cho LH, Antt HW, Koh HJ, An G (2017) KNOX protein OSH15 induces grain shattering by repressing lignin biosynthesis genes. Plant Physiol **174**: 312–325

Zhang D, Luo X, Zhu L (2011) Cytological analysis and genetic control of rice anther development. J Genet Genomics **38**: 379–390

Zhu L, Chu LC, Liang Y, Zhang XQ, Chen LQ, Ye D (2018) The Arabidopsis CrRLK1L protein kinases BUPS1 and BUPS2 are required for normal growth of pollen tubes in the pistil. Plant J **95**: 474–486